A Scaler-Based Data Acquisition System for Measuring Parity Violation Asymmetry in Deep Inelastic Scattering

R. Subedi,[1,2] X. Deng,[1] K. Pan,[3] D. Wang,[1] R. Michaels,[4] P. E. Reimer,[5] A. Shahinyan,[4] B. Wojtsekhowski,[4] and X. Zheng[1]

[1]*University of Virginia, Charlottesville, VA 22904, USA*
[2]*George Washington University, 725 21st St, NW, Washington, DC 20052, USA*
[3]*Massachesetts Institute of Technology, Cambridge, MA 02139, USA*
[4]*Thomas Jefferson National Accelerator Facility, Newport News, VA 23606, USA*
[5]*Argonne National Laboratory, Argonne, IL 60439, USA*

(Dated: September 20, 2010)

An experiment measuring the parity violating asymmetry in deep inelastic scattering was completed at the Thomas Jefferson National Accelerator Facility in experimental Hall A. From this asymmetry one can extract a combination of the product of the electron neutral weak vector coupling and the quark neutral weak axial coupling with a factor of six improvement in precision over world data. To achieve this, asymmetries at the 10^{-4} level were measured. A highly specialized data acquisition (DAQ) system with intrinsic particle identification was developed and utilized. The DAQ system of this experiment is presented here with an emphasis on understanding of its deadtime, pileup effects, and the capability of measuring small asymmetries.

PACS numbers: 21.10.Hw, 25.30.-c

Introduction

The Parity Violating Deep Inelastic Scattering (PVDIS) experiment E08-011 was completed in December 2009 at the Thomas Jefferson National Accelerator Facility (JLab). The goal of this experiment [1–3] is to measure to a high precision the parity violating asymmetry in deep inelastic scattering of a polarized electron beam on an unpolarized liquid deuterium target. This asymmetry is sensitive to the effective neutral weak coupling combination $2C_{2u} - C_{2d}$, where $C_{2q} = g_V^e g_A^q$ with $q = u, d$ indicating an up or a down quark, g_V^e is the electron vector coupling and g_A^q is the quark axial coupling.

For electron inclusive scattering from an unpolarized target, the electromagnetic interaction is parity conserving and is insensitive to the spin flip of the incoming electron beam. Only the weak interaction violates parity. Taking the difference of the left-handed and right-handed electron scattering cross-sections, one can isolate the parity violating contribution. The parity violating asymmetry for deep inelastic electron scattering from a deuterium target, A_{PV}, can be written as

$$\begin{aligned} A_{PV} &= \frac{\sigma_+ - \sigma_-}{\sigma_+ + \sigma_-} \\ &= \left(\frac{3G_F Q^2}{\pi\alpha^2\sqrt{2}}\right)\left(\frac{1}{5 + R_S(x) + 4R_C(x)}\right) \\ &\quad \times \{2C_{1u}[1 + R_C(x)] - C_{1d}[1 + R_S(x)] + \\ &\quad Y(2C_{2u} - C_{2d})R_V(x)\} \ , \end{aligned} \tag{1}$$

where σ_+ and σ_- are the left-handed and right-handed electron scattering cross-sections, respectively, Q^2 is the negative of the four-momentum transfer squared, G_F is the Fermi weak coupling constant, α is the fine structure constant, Y is a kinematic factor, $R_{S,C}$ and R_V are related to sea- and valence-quark distribution functions, and x is the Bjorken scaling variable (for details see Ref. [1, 2]). The magnitude of this asymmetry is approximately 100 ppm at $Q^2 = 1$ (GeV/c)^2. Within the context of the Standard Model, the effective weak coupling constants $C_{1,2q}$ are

$$\begin{aligned} C_{1u} &= g_A^e g_V^u = -\frac{1}{2} + \frac{3}{4}\sin^2\theta_W \ , \\ C_{2u} &= g_V^e g_A^u = -\frac{1}{2} + 2\sin^2\theta_W \ , \\ C_{1d} &= g_A^e g_V^d = \frac{1}{2} - \frac{2}{3}\sin^2\theta_W \ , \\ C_{2d} &= g_V^e g_A^d = \frac{1}{2} - 2\sin^2\theta_W \ , \end{aligned}$$

where θ_W is the weak mixing angle. The goal of the experiment is to measure the PVDIS asymmetries to a precision of $3 - 4\%$, and to extract from these asymmetries the effective coupling constant combination $(2C_{2u} - C_{2d})$. The magnitude of the asymmetry is expected to be between 90 and 170 ppm. To achieve the required precision, event rates up to 500 kHz are expected.

The experiment used a 100 μA polarized electron beam with a polarization of approximately 89% and a 20-cm long liquid deuterium target. The two High Resolution Spectrometers (HRS) [4] were used to detect scattered electrons. Similar to other deep inelastic scattering experiments, the main challenge of the measurement is how to separate electrons from charged pion background from electro- or photo-productions. While the standard detector package and the data acquisition (DAQ) system of the HRS provide routinely a high particle identification (PID) performance, they are based on full recording of the detector output signals and are limited to event rates of up to 4 kHz. This is not sufficient for the high rates expected for the PVDIS experiment. The high pion background also prohibited the use of integrating DAQs used by previous parity violation experiments at JLab. The design goal of the new DAQ is to count events rates up to 1 MHz with hardware-based PID.

Detector and Data Acquisition System

The following detectors in the HRS were used during this experiment: two scintillator planes to provide the main trigger, a CO_2 gas cherenkov counter and a double-layered lead glass counter to provide particle identification. The standard tracking detector (the vertical drift chamber) was turned off during production data taking because it cannot endure the expected high event rates.

For the gas cherenkov detector and the double-layered lead glass counter, a full recording of their output ADC spectrum is not feasible at high rate. Instead their output signals are passed through discriminators and logic units to form preliminary electron and pion triggers. These preliminary triggers are then combined with the scintillator triggers and cherenkov signals of the traditional DAQ to form the final electron and pion triggers, which are then sent to scalers to record the event rates and the asymmetries. The particle identification is fulfilled by the use of discriminators for both the lead-glass and the cherenkov counters and proper settings of their thresholds.

The two layers of the lead glass counter are called "preshower" and "shower" detectors, respectively. The preshower blocks in the HRS to the right side of the beamline when viewed along the beam direction (called the Right HRS) had 48 blocks arranged in a 2×24 array, with the longer dimension perpendicular to the particle trajectory. For the two bars in each row, only the ends facing outward are read out by photo-multiplier tubes (PMTs) and the other ends of the two bars were facing each other and not read out. Therefore the preshower detector had 48 output channels. All preshower blocks were individually wrapped to block light leak. The preshower and the shower detectors in the Left HRS are similar to the preshower detector on the Right HRS except that for each detector there are 34 blocks arranged in a 2×17 array. The shower detector in the Right HRS had 80 blocks arranged in a 5×15 array with their longer dimension along the trajectory of scattered particles, with a PMT attached to each block on one end only, giving 75 output channels. In order to reduce the amount of electronics needed and to avoid high electronic background, the lead blocks in both the preshower and the shower detectors are divided into 6 (8) groups for the Left (Right) HRS, with each group consisting 8 blocks. On the Right HRS only 60 of the 75 shower blocks were used while the 16 blocks in the 5^{th} column were not included in the DAQ. The effect on the HRS acceptance is negligible because the 5^{th} was on the edge of the acceptance. Signals from blocks in each group are added using a custom-made analog summing unit (SUM8), then passed to discriminators. The geometry and position of each pre-shower group was carefully chosen to match those of the corresponding shower group to maximize electron detection efficiency. On the Left HRS adjacent groups in both preshower and shower had overlapping blocks, while for the Right HRS only preshower blocks were overlapping. To allow overlapping between adjacent groups, signals from preshower on the Right HRS and both preshower

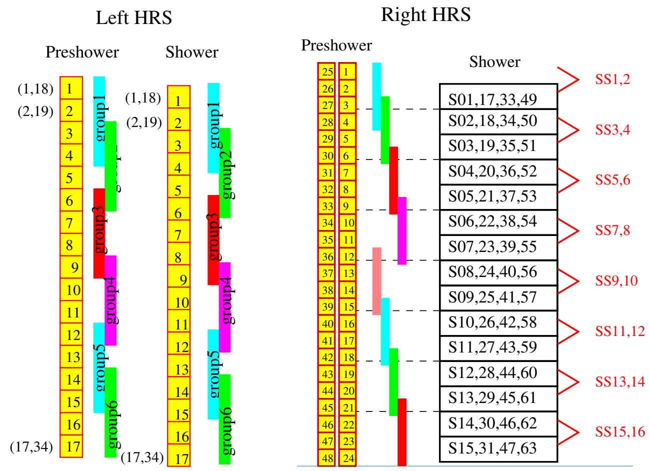

FIG. 1: Grouping scheme (side-view) for the double-layered lead glass counters for the new DAQ. The colored vertical bars represent the range of each group.

and shower on the Left HRS were split into two identical outputs using passive splitters. Grouping of the lead glass blocks (side-view) is shown in Fig. 1.

A schematic diagram for the DAQ electronics for the Right HRS is shown in Fig. 2. The electron and pion triggers were formed by passing shower (SS) and preshower (PS) signals or their sums, called total shower (TS) signals, through discriminators with different thresholds. For electron triggers, logical ANDs of the preshower discriminator and the total shower discriminator outputs were formed. For pion triggers only one set of discriminators were used on the total shower signals. These signals were then combined with the signal from scintillators and the gas cherenkov (called electron or pion "VETO" signals) to form electron or pion triggers for each shower and preshower group. The electron or pion triggers from all eight (six for the Left HRS) groups were then ORed together to form the final electron or pion triggers for the Left (Right) HRS. All triggers – electron and pions from each group, as well as the final triggers – were recorded using scalers.

In order to study the counting deadtime of the DAQ, two identical paths were constructed for each trigger. The only difference between the two paths is in the discriminator output width, which were set at 30 ns and 100 ns, for the narrow and the wide paths, respectively. Since scaler counting is free of deadtime effect and the output width of all logic modules were set to 15 ns, much narrower than the discriminator width, the deadtime of the DAQ is dominated by those from the discriminators.

The SUM8 modules used for summing all lead glass signals also served as fan-out modules, providing exact copies of the input PMT signals. These copies are sent to the traditional HRS DAQ, hence the traditional DAQ remained fully functional. During the experiment, data were collected at low rates using reduced beam currents with both DAQs functioning, such that a direct comparison of the two DAQs can be made. The vertical drift chamber was also used during these

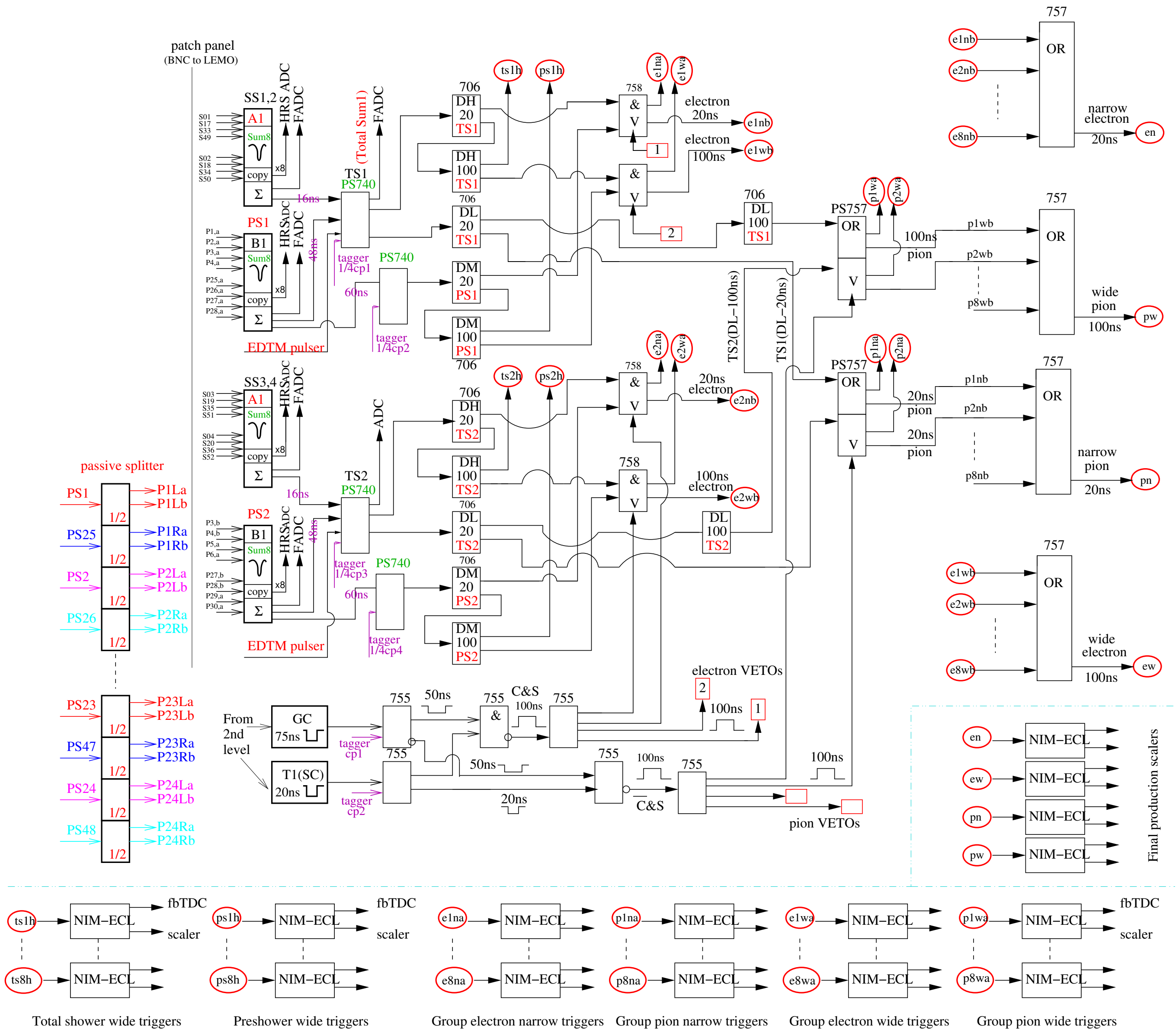

FIG. 2: Electronics diagram for the Right HRS DAQ used by the PVDIS experiment. The Sum8's, discriminators and logic modules for two groups are shown, as well as the location of the tagger signal, setup of the VETO circuit using the scintillator and the gas cherenkov signals, the logic units for combining triggers from all eight groups into final triggers, and the scalers. Electronics for the Left HRS are similar except the units related to grouping.

low rate DAQ studies. Outputs from all discriminators, signals from the scintillator and the gas cherenkov, and all electron and pion triggers were sent to fastbus TDCs (fbTDC) and were recorded in the traditional DAQ. Signals from these fbTDCs were used to align all signals in timing before the production data taking. They also allow the study of the cherenkov or lead-glass spectrum for the new DAQ triggers.

PID performance

PID performance of the new DAQ system were studied at a low beam current using fbTDC signals along with ADC spectrum of all detector signals recorded by the traditional DAQ. Figure 3 shows the preshower vs. shower signals for group 2 on the Left HRS, without fbTDC cut (left) and with cut on the fbTDC signal of the electron wide trigger from this group.

Electron efficiency and pion rejection factors of the lead glass counter on the Left HRS are shown in Fig. 4 as functions of the vertical hit position of the particle in the preshower detector. PID performance on the Right HRS is similar. Electron

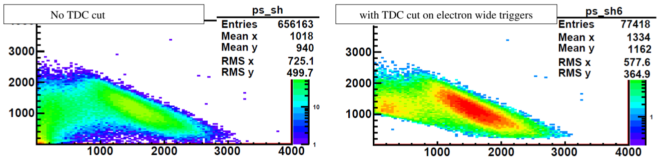

FIG. 3: Preshower vs. Shower ADC spectrum (sum of 8 blocks) for group 2 on the Left HRS, without fbTDC cut (left) and with cut on the electron wide trigger fbTDC signal. It clearly shows the hardware cuts on the shower and the total shower signals, indicating the DAQ is selecting the correct events as electrons. The cuts can be adjusted by changing the discriminator thresholds. The events near (200,1000) are electrons that deposited energy in overlapping blocks and are recorded in adjacent groups.

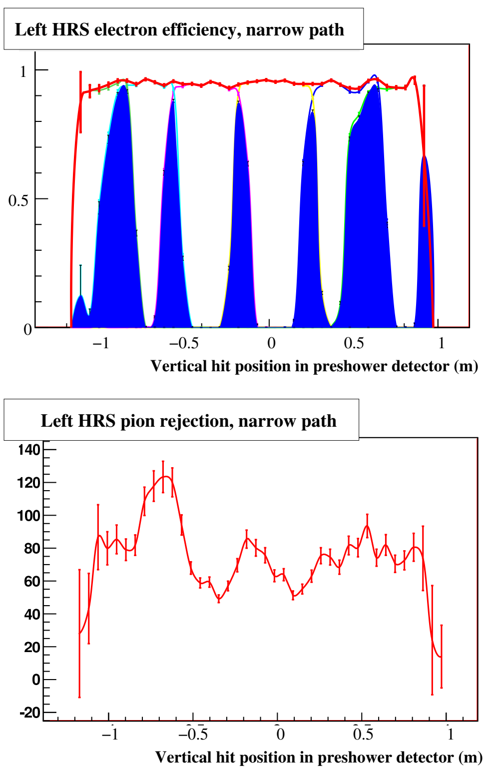

FIG. 4: Electron detection efficiency (top) and pion rejection factor (bottom) vs. vertical (dispersive) hit position of the particle in the preshower detector for the narrow electron triggers in the Left HRS. For electron efficiencies, the total efficiency is shown by the red curve, while blue shaded area indicates events that are recorded by the two adjacent groups. The average electron efficiency across the detector for the run (about 60 minutes long) used in this figure is $(94.626\pm0.002)\%$ and the averge pion rejection factor is 75.3 ± 1.1. The error bars are statistical only. PID performance for the wide path and the Right HRS are similar.

efficiency from wide groups are slightly higher than narrow groups because of the slight higher loss due to timing misalignment when ANDing the preshower and the total shower discriminator outputs.

Deadtime Study

Deadtime is the amount of time after an event during which the system is unable to record another event. Identifying exact value of the deadtime is always a challenge in counting experiments. To measure deadtime in this experiment, two different output widths were set for the discriminators for both electron and pion triggers: 30 ns ("narrow path") and 100 ns ("wide path"). All other electronic modules had 20 ns output widths such that the deadtime of the electronics is expected to be dominated by the discriminators. In addition, dividing lead glass blocks into groups help to greatly reduce the deadtime loss in each group compared to summing all blocks together and forming only one final trigger.

In order to study the deadtime in details, a high rate pulser signal (called "tagger") was combined with all preshower and total shower signals using analog summing modules, see Figs. 2 and 5. In the absence of all detector signals, the tagger produces without loss electron triggers and "tagger coincidence" signals. When high-rate detector signals are present, however, the recorded tagger coincidence rates would be affected by the DAQ deadtime. The relative loss in the tagger coincidence output w.r.t. the tagger input is determined by:

1. The deadtime loss: when a PMT signal precedes the tagger signal by a time interval that is less than the deadtime but longer than the delayed tagger signal width, the tagger signal could be lost and no coincidence output is formed;

2. The pileup effect: when a PMT signal precedes the tagger signal by a time interval that is shorter than both the deadtime and the delayed tagger signal width, there could be coincidence output between the delayed tagger and the trigger caused by the PMT signal even though the tagger should have been lost due to deadtime. This pileup effect can be measured because in this case the delay between the coincidence output and the input tagger would be smaller than when the trigger is caused by the tagger. This effect is illustrated in Fig. 5 and contributes to both I_1 and I_2 region of the fbTDC spectrum.

The fractional loss of tagger events due to deadtime can be measured as

$$D = 1 - (1-p)(R_o/R_i),$$

where R_i is the input tagger rate, R_o is the output coincidence signal rate, and $p = (I_1 + I_2)/I_0$ is a correction factor for pileup effects (see Fig. 5 for definition of $I_{0,1,2}$). The pileup effect was measured using fbTDC spectrum for electron narrow and wide triggers for all groups. Results for the deadtime loss D are shown in Fig. 6 vs. rates of PMT signals from scattered particles. Different beam currents between 20 and 100 μA were used in this deadtime measurement.

The slope of the deadtime loss vs. rate plot gives the value of deadtime in seconds. From Fig. 6 one can see that the deadtime for the wide path is approximately 100 ns as expected.

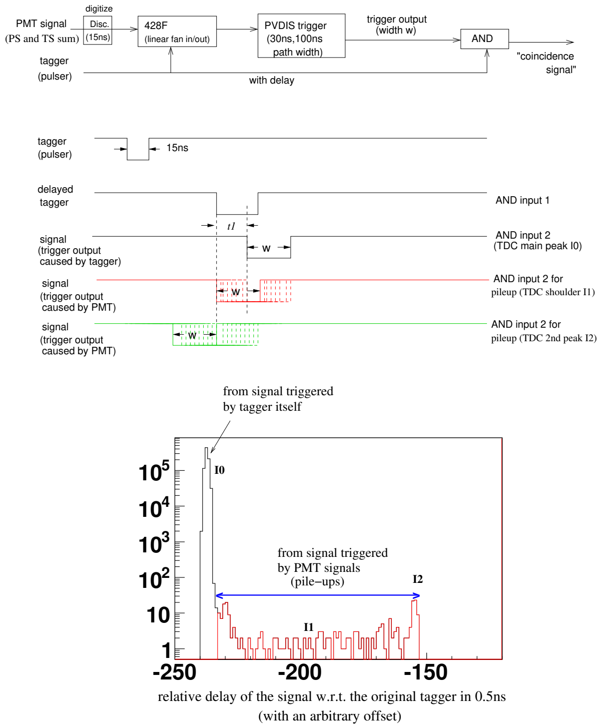

FIG. 5: Schematic diagram for the tagger setup and it's timing sequence. A typical fbTDC spectrum for the relative timing between the output coincidence signal and the input tagger is shown in the bottom. Two different scenarios are shown: 1) when there is no PMT signal preceding the tagger, the tagger triggers the DAQ and forms a coincidence signal with the delayed tagger. This forms the main peak I_0 in the fbTDC spectrum; 2) when there is a PMT signal preceding the tagger by a time interval shorter than the delayed tagger width, the PMT signal triggers the DAQ and forms a coincidence signal with the delayed tagger. This forms the pileup area I_1 and I_2.

The deadtime for the narrow path, on the other hand, is dominated by the input PMT signal width (typically 60-80 ns) instead of the 30-ns discriminator width. Because the VETO circuit – the electronics that used scintillator and cherenkov signals to form "gate" signals for the electron and pion triggers from the lead-glass detector – is designed to be free of deadtime, the deadtime loss measured using tagger signals is the deadtime loss of the physics events.

The absolute deadtime loss gives a direct correction to the measured asymmetry. The rates during production data taking at this kinematics were between 8 and 9 kHz for the groups shown, which had the highest rates among all groups of the HRS. Since the deadtime loss was at a level of 0.1% and was measured to a 1.2% relative level, as shown in Fig. 6, the uncertainty on the final asymmetry due to deadtime loss at this kinematics is therefore negligible compared to the expected 4% statistical uncertainty.

This experiment had two kinematics: $Q^2 = 1.1$ and 1.9 (GeV/c)^2. The deadtime loss at the $Q^2 = 1.1$ (GeV/c)^2 point were higher due to higher rates, but was also measured to a $\approx 1\%$ relative level and the uncertainty of the measured asymmetry is again negligible compared to the expected 3% statistical uncertainty.

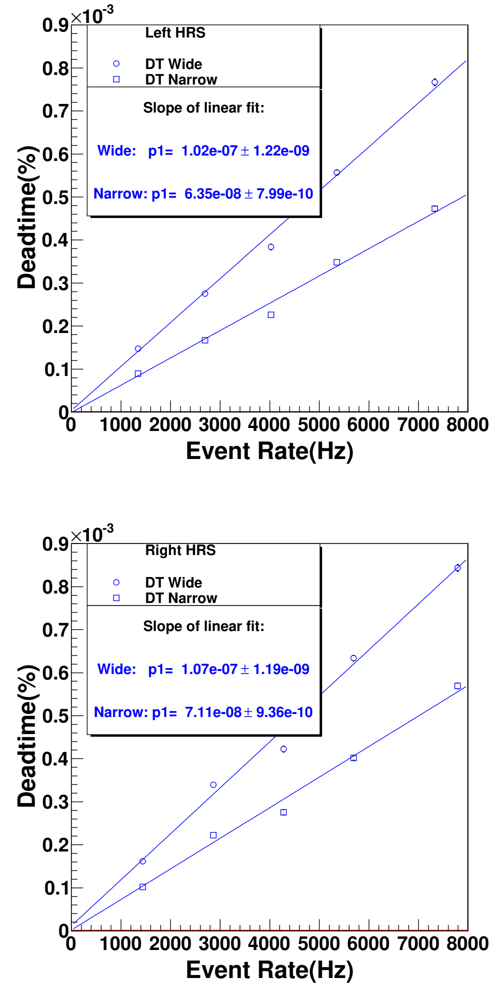

FIG. 6: Deadtime loss in percent vs. event rate for group 3 on the Left HRS (top) and for group 4 on the Right HRS (bottom). These data were taken at a Q^2 of 1.9 (GeV/c)^2. The two groups shown are from the central blocks of the shower and preshower detectors and had the highest rates among all groups of each HRS.

Pileup in DAQ

Trigger Simulation

Although the deadtime loss of each group was measured using tagger signals to a high precision, there was no direct measurement of the deadtime loss of the final electron trigger ("OR" of all groups). Instead an estimate of the final electron trigger deadtime loss is provided by a simulation that takes into account of all electronics of the DAQ. ??? ???

FIG. 7: Counting asymmetry for group ??? on the Left HRS from 1 M beam helicity pairs (each pair is 66 ms).

Asymmetries

The physics asymmetry sought for in this experiment was between 90 and 170 ppm. Figure 7 shows the counting asymmetry collected by the DAQ for 1 M beam helicity pairs where one pair corresponds to 66 ms of beam. One can see that the asymmetry spectrum agrees well with the expected Gaussian distribution. To understand further systematics of the asymmetry measurement, a half-wave plate (HWP) was inserted in the beamline to flip the laser helicity in the polarized source during half of the data taking period. The measured asymmetries flip sign for each beam HWP change and the magnitude of the asymmetry remain consistent within statistical error bars.

Conclusion

The newly developed scaler-based counting DAQ was successfully implemented in the 6 GeV PVDIS experiment at Jefferson Lab. Asymmetries measured by the DAQ agree with Gaussian distribution. Particle identification performance and counting deadtime of the DAQ were measured during the experiment and results are well understood. The deadtime loss of the PVDIS electronics was found to be below ???% and was understood to better than ??? %.

[1] R. Michaels, P. Reimer, X.-C. Zheng, et al., $\vec{e}$–^2h *parity violating deep inelastic scattering at cebaf 6 GeV* (2005), JLab PR05-007.

[2] R. Michaels, P. Reimer, X.-C. Zheng, et al., $\vec{e}$–^2h *parity violating deep inelastic scattering (pvdis) at cebaf 6 GeV* (2008), JLab E08-011.

[3] R. Subedi, AIP proceedings of the 18th International Spin Physics Symposium p. 245 (2009).

[4] J. Alcorn et al., Nucl. Instrum. Meth. **A522**, 294 (2004).